IMPLEMENTING MULTI-SCALE AGRICULTURAL INDICATORS EXPLOITING SENTINELS

VEGETATION FIELD DATA AND PRODUCTION OF GROUND-BASED MAPS:

"CAPITANATA SITE, ITALY" 17TH MARCH AND 23RD APRIL, 2015

ISSUE I1.00

EC Proposal Reference N° FP7-311766

Actual submission date : June 2016

Start date of project: 01.11.2012 Duration : 40 months

Name of lead partner for this deliverable: EOLAB

Book Captain: Consuelo Latorre (EOLAB)

Contributing Authors: D. Vinué, F. Camacho (EOLAB)

A. Castrignanò, S. Ruggieri, C. Riefolo, M. Tomaiulolo, P. Campi, D. Ventrella and A.V. Vonella (CRA-SCA)
M. Rinaldi, (CRA-CER), P. Toscano (CNR-IBIMET)
G. Buttafuoco (CNR-ISAFOM)

Project co-funded by the European Commission within the Seventh Framework Program (2007-2013)		
Dissemination Level		
PU	Public	**X**
PP	Restricted to other programme participants (including the Commission Services)	
RE	Restricted to a group specified by the consortium (including the Commission Services)	
CO	Confidential, only for members of the consortium (including the Commission Services)	

DOCUMENT RELEASE SHEET

Book Captain:	C. Latorre	Date: 08.06.2016	Sign.
Approval:	R. Lacaze	Date: 17.06.2016	Sign.
Endorsement:	M. Koleva	Date:	Sign.
Distribution:	Public		

CHANGE RECORD

Issue/Revision	Date	Page(s)	Description of Change	Release
	08.06.2016	All	First Issue	I1.00

TABLE OF CONTENTS

LIST OF FIGURES

LIST OF TABLES

LIST OF ACRONYMS

CEOS	Committee on Earth Observation Satellite
CEOS LPV	Land Product Validation Subgroup
CER	Cereal Research Centre (Italy)
CNR	*Consiglio Nazionale delle Ricerche* - National Research Council (Italy)
CRA	Council for Agricultural Research and Agricultural Economy Analysis (Italy)
DG AGRI	Directorate General for Agriculture and Rural Development
DG RELEX	Directorate General for External Relations (European Commission)
ECV	Essential Climate Variables
EUROSTATS	Directorate General of the European Commission
ESU	Elementary Sampling Unit
FAPAR	Fraction of Absorbed Photo-synthetically Active Radiation
FAO	Food and Agriculture Organization
GCOS	Global Climate Observing System
GEO-GLAM	Global Agricultural Geo- Monitoring Initiative
GIO-GL	GMES Initial Operations - Global Land (GMES)
GCOS	Global Climate Observing System
GMES	Global Monitoring for Environment and Security
GPS	Global Positioning System
IBIMET	Institute of Biometeorology
IMAGINES	Implementing Multi-scale Agricultural Indicators Exploiting Sentinels
ISAFOM	Istituto per i sistemi Agricoli e Forestali del Mediterraneo
JECAM	Joint Experiment for Crop Assessment and Monitoring
LAI	Leaf Area Index
LDAS	Land Data Assimilation System
LUT	Look-up-table techniques
PROBA-V	Project for On-Board Autonomy satellite, the V standing for vegetation.
RMSE	Root Mean Square Error
SPOT /VGT	Satellite Pour l'Observation de la Terre / VEGETATION
SCA	Unità di Ricerca per I Sistemi Colturali degli Ambienti caldo-aridi
SCI	GMES Services Coordinated Interface
SLT	Solar Local Time
TOC	Top of Canopy Reflectance
USGS	U.S. Geological Survey Science organization.
UTM	Universal Transverse Mercator coordinates system
VALERI	Validation of Land European Remote sensing Instruments
WGCV	Working Group on Calibration and Validation (CEOS)

1. BACKGROUND OF THE DOCUMENT

1.1. Executive Summary

The Copernicus Land Service has been built in the framework of the FP7 geoland2 project, which has set up pre-operational infrastructures. ImagineS intends to ensure the continuity of the innovation and development activities of geoland2 to support the operations of the global land component of the GMES Initial Operation (GIO) phase. In particular, the use of the future Sentinel data in an operational context will be prepared. Moreover, IMAGINES will favor the emergence of new downstream activities dedicated to the monitoring of crop and fodder production.

The main objectives of ImagineS are to (i) improve the retrieval of basic biophysical variables, mainly LAI, FAPAR and the surface albedo, identified as Terrestrial Essential Climate Variables, by merging the information coming from different sensors (PROBA-V and Landsat) in view to prepare the use of Sentinel missions data; (ii) develop qualified software able to process multi-sensor data at the global scale on a fully automatic basis; (iii) complement and contribute to the existing or future agricultural services by providing new data streams relying upon an original method to assess the above-ground biomass, based on the assimilation of satellite products in a Land Data Assimilation System (LDAS) in order to monitor the crop/fodder biomass production together with the carbon and water fluxes;(iv) demonstrate the added value of this contribution for a community of users acting at global, European, national, and regional scales.

Further, ImagineS serves the growing needs of international (e.g. FAO and NGOs), European (e.g. DG AGRI, EUROSTATS, DG RELEX), and national users (e.g. national services in agro-meteorology, ministries, group of producers, traders) on accurate and reliable information for the implementation of the EU Common Agricultural Policy, of the food security policy, for early warning systems, and trading issues. ImagineS will also contribute to the Global Agricultural Geo-Monitoring Initiative (GEO-GLAM) by its original agriculture service which can monitor crop and fodder production together with the carbon and water fluxes and can provide drought indicators, and through links with JECAM (Joint Experiment for Crop Assessment and Monitoring).

1.2. Portfolio

The ImagineS portfolio contains global and regional biophysical variables derived from multi-sensor satellite data, at different spatial resolutions, together with agricultural indicators, including the above-ground biomass, the carbon and water fluxes, and drought indices resulting from the assimilation of the biophysical variables in the Land Data Assimilation System (LDAS).

The production in Near Real Time of the 333m resolution products, at a frequency of 10 days, using PROBA-V data is carried out in the Copernicus Global Land Service. (http://land.copernicus.eu/global/).

The demonstration of high resolution (30m) products derived from Landsat-8 was done over demonstration sites of cropland and grassland in contrasting climatic and environmental conditions. Demonstration products are available on the ImagineS website (http://www.fp7-imagines.eu/pages/services-and-products/landsat-8-biophysical-products.php).

1.3. Scope and Objectives

The main objective of this document is to describe the field campaign and ground data collected at Capitanata, in Italy, and the up-scaling of the ground data to produce ground-based high resolution maps of the following biophysical variables:

- Leaf Area Index (LAI), defined as half of the total developed area of leaves per unit ground surface area (m^2/m^2). We focused on two different LAI quantities (for green elements):
    - The effective LAI (LAIeff) derived from the description of the gap fraction as a function of the view zenith angle.
    - The actual LAI (LAI) estimate corrected from the clumping index.
- Fraction of Absorbed Photosynthetically Active Radiation (FAPAR), which is the fraction of the photosynthetically active radiation (PAR) absorbed by a vegetation canopy. We are also focused on green elements. PAR is the solar radiation reaching the canopy in the 0.4–0.7 µm wavelength region. FAPAR was estimated from LAI measurements using the Beer's law, and empirical coefficients.

1.4. Content of the Document

This document is structured as follows:

- Chapter 2 provides an introduction to the field experiment.
- Chapter 3 provides the location and description of the site.
- Chapter 4 describes the ground measurements, including material and methods, sampling and data processing.
- Chapter 5 provides an evaluation of the sampling.
- Chapter 6 describes the production of high resolution ground-based maps, and the selected "mean" values for validation.

1.5. Related Document

- ImagineS_RP7.5_FieldCampaign_Capitanata2014: Field campaign and Data Processing report of the measurements collected in 2014 over Capitanata site.

2. INTRODUCTION

Validation of remote sensing products is mandatory to guaranty that the satellite products meets the user's requirements. Protocols for validation of global LAIeff products are already developed in the context of Land Product Validation (LPV) group of the Committee on Earth Observation Satellite (CEOS) for the validation of satellite-derived land products (Fernandes et al., 2014), and recently applied to Copernicus global land products based on SPOT/VGT observations (Camacho et al., 2013). This generic approach is made of 2 major components:

- The indirect validation: including inter-comparison between products as well as evaluation of their temporal and spatial consistency
- The direct validation: comparing satellite products to ground measurements of the corresponding biophysical variables. In the case of low and medium resolution sensors, the main difficulty relies on scaling local ground measurements to the extent corresponding to pixels size. However, the direct validation is limited by the small number of sites, for that reason a main objective of ImagineS is the collection of ground truth data in demonstration sites.

The content of this document is compliant with existing validation guidelines (for direct validation) as proposed by the CEOS LPV group (Morisette et al., 2006); the VALERI project (http://w3.avignon.inra.fr/valeri/) and ESA campaigns (Baret and Fernandes, 2012). It therefore follows the general strategy based on a bottom up approach: it starts from the scale of the individual measurements that are aggregated over an elementary sampling unit (ESU) corresponding to a support area consistent with that of the high resolution imagery used for the up-scaling of ground data. Several ESUs are sampled over the site. Radiometric values over a decametric image are also extracted over the ESUs. This will be later used to develop empirical transfer functions for up-scaling the ESU ground measurements (e.g. Martínez et al., 2009). Finally, the high resolution ground based map will be compared with the medium resolution satellite product at the spatial support of the product.

One of the JECAM sites, "Italy Apulian Tavoliere" is located in Capitanata area, Italy. The experimental farm is managed by CNR-SCA (*Consiglio Nazionale delle Ricerche - Unità di Ricerca per I Sistemi Colturali degli Ambienti caldo-aridi*). CNR-SCA collaborated with ImagineS project, providing four field campaigns (two per year) in 2014 (Latorre et al, 2016) and 2015 (this report).

During 2015, two field campaigns were carried out in March and April. A set of ground-truth LAI measurements, soil and crop data type were collected in order to: 1) calibrate a simulation model of crop growth and production; 2) test of multivariate geostatistical method of data fusion by which leaf area index(LAI), FIPAR and crop height can be predicted from a set of ground-truth measurements and using remote sensing multiband images as auxiliary variables; 3) explore the potential of ESA Sentinel-1 satellite for its use in agriculture (JECAM, 2015).

This report describes the ground dataset provided by CRA-SCA. EOLAB has up-scaled the ground dataset using the ground data and TOC reflectance imagery. Only the second campaign was up- scaled (no cloud free Landsat imagery available for the first campaign).

Field Campaigns:

- **First campaign:** 17th to 20th of March, 2015
- **Second campaign:** 9th to 23th of April, 2015 (Up-scaled)

Contact:

- CRA – SCA Bari: Annamaria Castrignanò, Sergio Ruggieri, Domenico Ventrella, and Pasquale Campi.

- CRA-CER Foggia: Michele Rinaldi.

- CNR-IBIMET Florence: Piero Toscano.

- CNR-ISAFOM Rende (Cosenza): Gabriele Buttafuoco.

3. STUDY AREA

3.1. LOCATION

The field campaign is located on “Capitanata area”, a plain of about 4000 km^2 located in the northern part of Apulia Region (south-eastern Italy), province of Foggia (Figure 1). “Capitanata” plain is delimited by the Apennines Chain west and by Gargano Promontory east and is mostly constituted by continental and fluvial sediments and some terraced marine deposits of the Pliocene and Pleistocene ages.

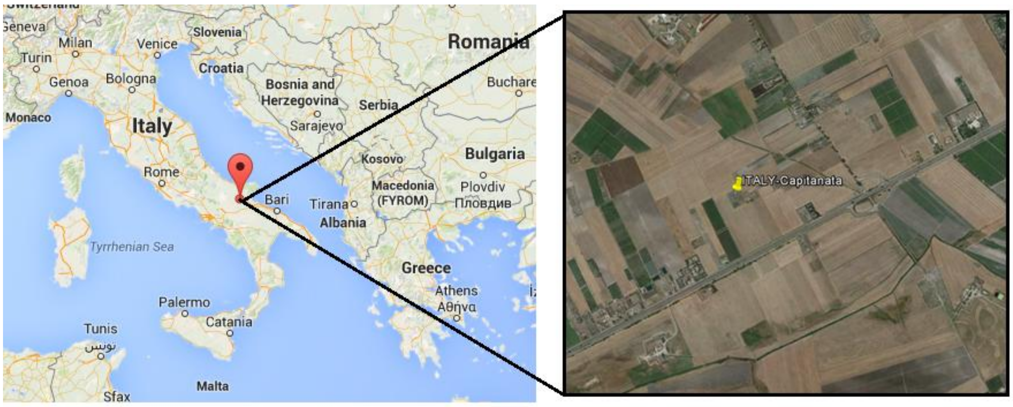

Figure 1: Location of Capitanata site in Italy.

Table 1: Coordinates and altitude of the test site (centre).

CAMPAIGN	Altitude	Latitud	Longitude
Capitanata	90m	41.4637º N	+15.4867º E

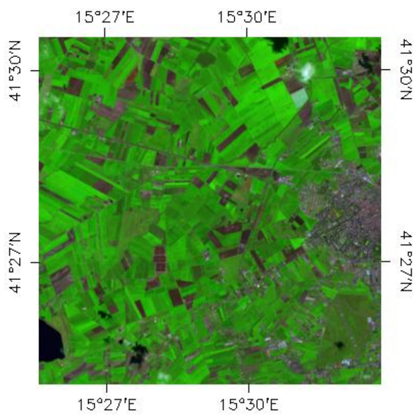

Figure 2: False color composition (SWIR-NIR-RED) of TOC Reflectance Landsat-8 images over the study area 10 km^2. (Capitanata, 23rd April, 2015).

Figure 2 shows the false color composition (RGB – SWIR-NIR-RED) over a Top Of Canopy (TOC) Reflectance Landsat-8 image used for up-scaling the ground dataset for the second campaign.

3.2. DESCRIPTION OF THE TEST SITE

This area is characterized by farms with average size up to 20 ha, highly productive soils cultivated under instensive and irrigated regime. Winter durum wheat (Triticum durum L.) represents the main cereal crop often grown in rotations with irrigated horticultural species. Among these, processing tomato crop (Lycopersicon aesculentum Mill.) is well represented. In particular, two-year rotation (tomato-wheat) and three – year rotation (tomato-wheat-wheat) are the typical farming rotations of this important productive area (for more details see Latorre et al, 2016; JECAM, 2014).

The climate of this zone is classified as “Accentuated Thermo- Mediterranean” (UNESCO-FAO), with winter seasons characterized by temperatures that sometimes descend below 0°C and hot summers with temperature that may exceed 40°C. Annual precipitation ranges between 400 and 800 mm, mostly concentrated in winter months. The rainiest months are October and November, while the dry period is from May to September. In general, the soils are deep and clay with vertical behaviour, characterized by large and deep cracks in summer season under rain fed conditions. A wide part of the area is served by an irrigation consortium that fulfils the water requirements of crops with spring-summer cycle (e.g. tomato). In other parts, the irrigation for spring crops is carried out by utilizing private wells. The water table is very deep (200-300 m) (JECAM, 2015).

4. GROUND MEASUREMENTS

The ground measurement database reported here was acquired by several groups from Italy: CNR-SCA, CRA-CER, CNR-IBIMET and CNR-ISAFOM.

4.1. Material and Methods

Effective LAI (LAIeff): Effective Leaf area index (LAIeff) is defined as the total one-sided leaf area per unit ground surface area (m^2 m-^{2}). LAIeff was measured with LAI-2000 Plant Canopy Analyzer (LI-COR Inc., 2013) (See 4.1.1) which uses a fish-eye lens with a hemispheric field of view (± 45°). The detector is composed of five concentric rings (sensitive to radiation in the 320-490 nm range). Each ring responds over a different range of zenith angles and radiation is thus azimuthally integrated. The measurements were collected in one sensor mode using a 45° view cap, in clear sky condition, to avoid interferences from users' shadow.

This equipment measures the LAIeff by means of gap fraction, using above and below canopy light measurements.

LAI: The actual LAI that can be measured only with a planimeter with however possible allometric relationships to reduce the sampling, is related to the effective leaf area index through:

$$LAI_{eff} = C_f \cdot LAI \qquad \text{Eq. (1)}$$

where C_f is the clumping index (Lang, 1986 and 1987), (Nilson, 1971).

The LAIeff was used to derive the clumpling factor (C_f) using an empirical relationship for the study area based on the modified Beer's law (Rinaldi and Garofalo, 2011). In order to apply the Eq.2, a light extinction coefficient (k) defined as the slope of regression between the natural logarithm of diffuse non-intercepted sky radiation and LAI was calculated, both measured with a LI-COR LAI 2000 (k value resulted = 0.75).

$$Cf = k + (0.25) * \left(1 - e^{(-0.35 * LAI_{eff})}\right) \qquad \text{Eq. (2)}$$

Intercepted PAR: The photosynthetic active radiation (PAR) intercepted by the canopy was estimated using the following equation:

$$iPAR = PAR \cdot IE \qquad \text{Eq. (3)}$$

Global solar radiation (Rg 300-2500 nm) was derived from a pyranometer located in the local climatic station using the value recorded at the same time when the LAI was measured. PAR is equal to 0.48xRg

FAPAR: As there is little scattering by leaves in that particular spectral domain due to the strong absorbing features of the photosynthetic pigments, FAPAR is often assumed to be equal to FIPAR (Fraction of Intercepted Photosynthetically Active Radiation), and therefore directly related to the gap fraction. The FIPAR was estimated according to Rinaldi and Garofalo (2011), where IE is the interception efficiency of the canopy, calculated with Beer's law, as:

$$IE = FIPAR = 1 - e^{(k * LAI_{eff} * Cf)} \quad \text{Eq. (4)}$$

The coefficient of extinction (k) and the clumping (Cf) were derived as described above.

The following data is provided in the associated file: Effective LAI, LAI, Cf (clumping factor), FAPAR, Solar Global Radiation (Rg), PAR, among other information related to the stage and description of the ESUs. The uncertainty for LAI corresponds to the standard deviation of the measurements (see associated ***2015_VGM_Capitanata.xls*** *file).*

4.1.3 LI-COR LAI-2000C plant canopy analyser

The LAI-2000C (LI-COR Inc.2013) is a model of plant canopy analyser used in the field campaign (Figure 3).

Figure 3: LAI-2000C device.

These instruments calculate Leaf Area Index (LAI) and other canopy attributes from light measurements made with a "fish-eye" optical sensor (148º field-of-view). Measurements made above and below the canopy are used to calculate canopy light interception at five zenith angles (Figure 4). The average probability of light penetration into the canopy is computed by

$$\overline{P(\theta_i)} = \frac{1}{N_{obs}} \sum_{j=1}^{N_{obs}} \frac{B_{ij}}{A_{ij}} \quad \text{Eq. (5)}$$

where the subscript *i* (*i* = 1 … 5) refers to the optical sensor rings centered at θ_i and *j* refers to the number of observational pairs (*j* = 1 … N_{obs}). B_{ij} and A_{ij} are the j^{th} below and above canopy readings, respectively, for the i^{th} ring. The gap fraction for the i^{th} ring is computed from

$$G_i = e^{\left(\overline{\ln P(\theta_i)}\right)} = e^{\left(\frac{1}{N_{obs}}\sum_{j=1}^{N_{obs}} \ln \frac{B_{ij}}{A_{ij}}\right)} \qquad \text{Eq. (6)}$$

Assuming the foliage elements are randomly distributed in space, the effective PAI (PAIeff) can be estimated by the transmittance in the different view angles based on Miller's formula (Miller, 1967).

$$PAI_{eff} = 2\int_0^{\pi/2} -\ln P(\theta)\cos\theta\sin\theta d\theta \qquad \text{Eq. (7)}$$

The amount of foliage in a vegetative canopy can be deduced from measurements of how quickly radiation is attenuated as it passes through the canopy. By measuring this attenuation at several angles from the zenith, foliage orientation information can also be obtained. The LAI-2000 measures the attenuation of diffuse sky radiation at five zenith angles simultaneously, arranged in concentric rings.

A normal measurement with the LAI-2000 consists of a minimum of ten numbers: five of the numbers are the signals from the five detectors when the optical sensor was above the vegetation, and the remaining five are the readings made with the sensor below the vegetation. For both readings, the sensor is looking up at the sky. Five values of canopy transmittance are calculated from these readings by dividing corresponding pairs.

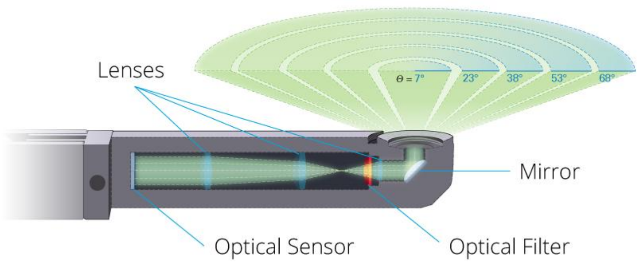

Figure 4: LAI-2000 optical sensor with 5 zenith angles

4.2. SPATIAL SAMPLING SCHEME

A pseudo-regular sampling was used within each Elementary Sampling Unit (ESU) of approximately 10m by 10m size within a polygon of 3 km by 3 km size. The two surveys were carried out on 17-20 March and 23-24 April, 2015.

For each ESU, the measurement was performed once above the canopy, to obtain reference values, and four times below the canopy, before being averaged out. The four measurements were carried out at the corners of 10m x 10m squares, whose centre georeferenced was used as representative of the ESU where the measurements were performed. The standard error of the four LAI measurements is also given in the instrument output (JECAM, 2014)

For each ESU, the measurement was performed once above the canopy, to obtain reference values, and four times below the canopy, before being averaged out. The four measurements were carried out at the corners of 10m x 10m squares, whose centre georeferenced was used as representative of the ESU where the measurements were performed. The standard error of the four LAI measurements is also given in the instrument output.

Figure 5 shows some pictures for three different crops (Durum wheat, chickpea and bean fields), taken during the two field campaigns. The second campaign carried out on April was performed at the end of the growing stage. Full covers are appreciated. Mainly wheat fields were monitored and provided in the dataset. In the second campaign on April, the only modification in land use is due to the change of bare soil that was replaced by processing tomato crop.

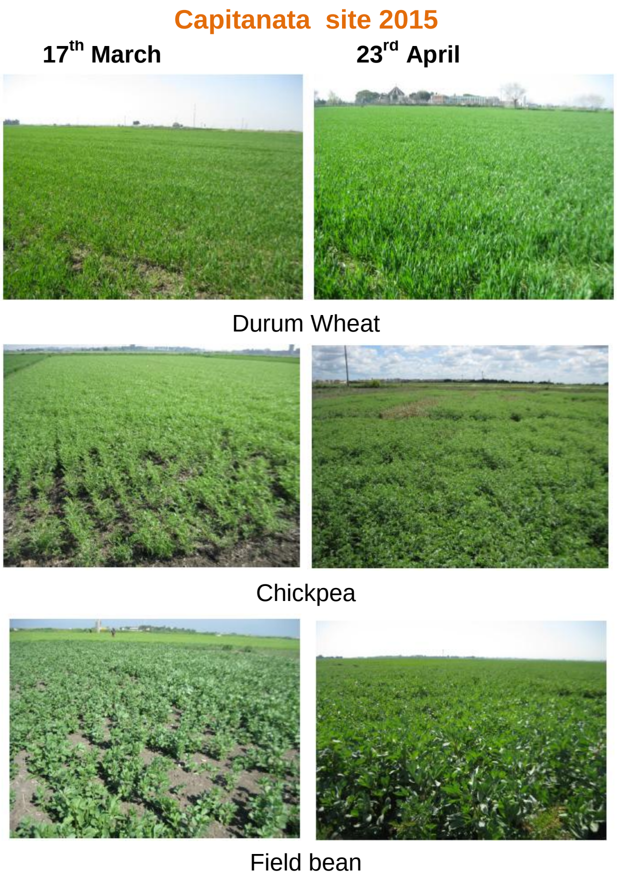

Figure 5: Photos of wheat, chickpea and field bean crop in March (left) and April (right) 2015.

The sampling area is located in the middle of Capitanata plain and has a flat topography (avg. altitude 90 m). Figure 6 shows the sampling for the two campaigns at two phenological stages (jointing and heading) of durum wheat.

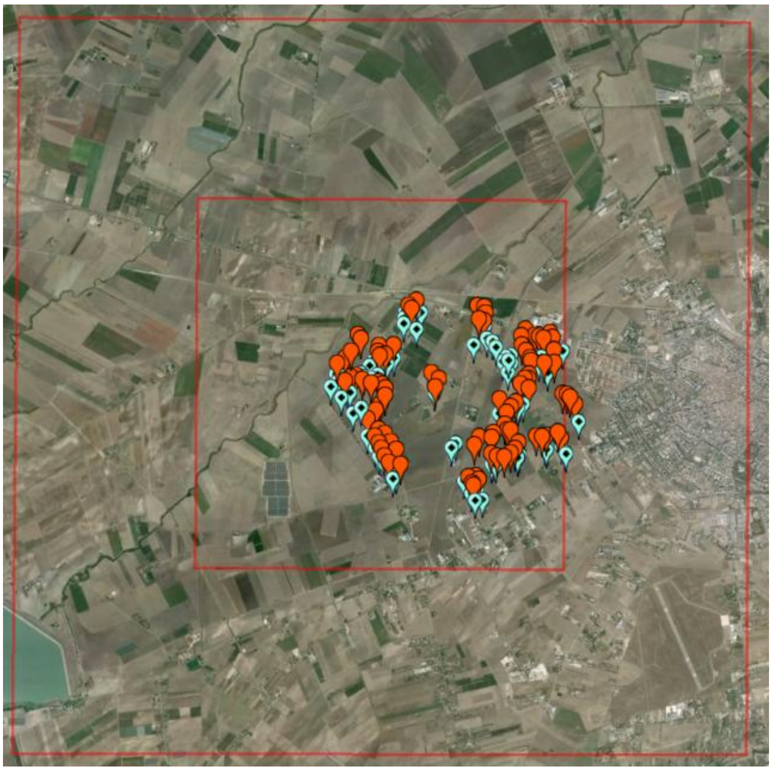

Figure 6: Spatial sampling over the study area of Capitanata site located in Italy during the 2015 year. Orange dots are the sampled ESUs of the first campaign, the blue dots are the sampled ESU of the second campaign.

4.3. GROUND DATA

4.3.1. Data processing

The dataset for the two field campaigns was processed although only the ground data for the second campaign (April, 2015) has been up-scaled due to the low quality of the TOC Landsat-8 image for the first one due to some clouds and shadows over the test area.

Figure 7 shows the intercomparison between LAI and effective LAI with instantaneous FAPAR. The exponential trend according to Beer's law is observed.

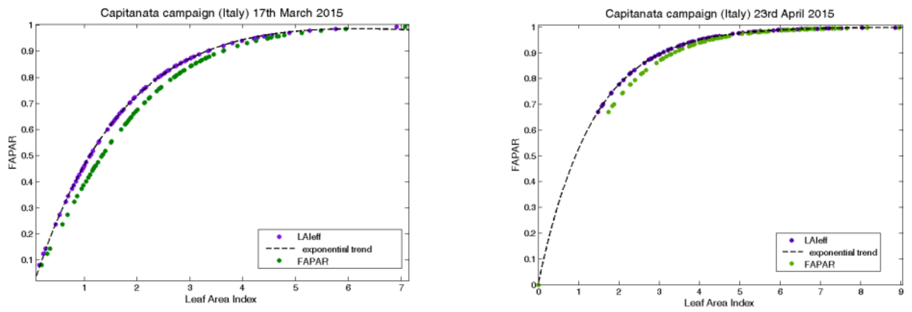

Figure 7: Intercomparison of the measured biophysical variables over the ESUs. Effective LAI and LAI versus FAPAR, Capitanata site (Italy). Left side: First field campaign (17th March). Right side: Second field campaign (23rd April).

4.3.2. Content of the Ground Dataset

Each ESU is described according to a standard format. The header of the database is shown in Table 2.

Table 2: The Header used to describe ESUs with the ground measurements.

<table>
<tr><th>Column</th><th colspan="2">Var.Name</th><th>Comment</th></tr>
<tr><td>1</td><td colspan="2">Plot #</td><td>Number of the field plot in the site</td></tr>
<tr><td>2</td><td colspan="2">Plot Label</td><td>Label of the plot in the site</td></tr>
<tr><td>3</td><td colspan="2">ESU #</td><td>Number of the Elementary Sampling Unit (ESU)</td></tr>
<tr><td>4</td><td colspan="2">ESU Label</td><td>Label of the ESU in the campaign</td></tr>
<tr><td>5</td><td colspan="2">Northing Coord.</td><td>Geographical coordinate: Latitude (º), WGS-84</td></tr>
<tr><td>6</td><td colspan="2">Easting Coord.</td><td>Geographical coordinate: Longitude (º), WGS-84</td></tr>
<tr><td>7</td><td colspan="2">Extent (m) of ESU (diameter)</td><td>Size of the ESU (1)</td></tr>
<tr><td>8</td><td colspan="2">Land Cover</td><td>Detailed land cover</td></tr>
<tr><td>9</td><td colspan="2">Start Date (dd/mm/yyyy)</td><td>Starting date of measurements</td></tr>
<tr><td>10</td><td colspan="2">End Date (dd/mm/yyyy)</td><td>Ending date of measurements</td></tr>
<tr><td>11</td><td rowspan="4">Products*</td><td>Method</td><td>Instrument</td></tr>
<tr><td>12</td><td>Nb. Replications</td><td>Number of Replications</td></tr>
<tr><td>13</td><td>PRODUCT</td><td>Methodology</td></tr>
<tr><td>14</td><td>Uncertainty</td><td>Standard deviation</td></tr>
</table>

*LAIeff, LAI and FAPAR

Figure 8 shows the obtained ground values for each ESU. For the first campaign, on March, low values were obtained for early heterogeneous wheat crops (ESU 19, ESU35). Other wheat fields as (ESU 9, 10 or 39) presented higher values ranging between 4 and 7 for LAIeff, and around 0.97-0.99 for FAPAR. Intermediate values were found for other canopies such as checkpea and bean fields.

Figure 9 describes the biophysical parameters obtained during the second campaign, the highest values were found for wheat and barley plots (ESU 22, 29-31) with LAIeff up to 8, and FAPAR values ranging between 0.99 and 0.1.

Note that additional ESU control points (ECP) were selected by visual inspection (LAIeff, LAI, FAPAR estimated equal to zero, bare, water and urban areas).

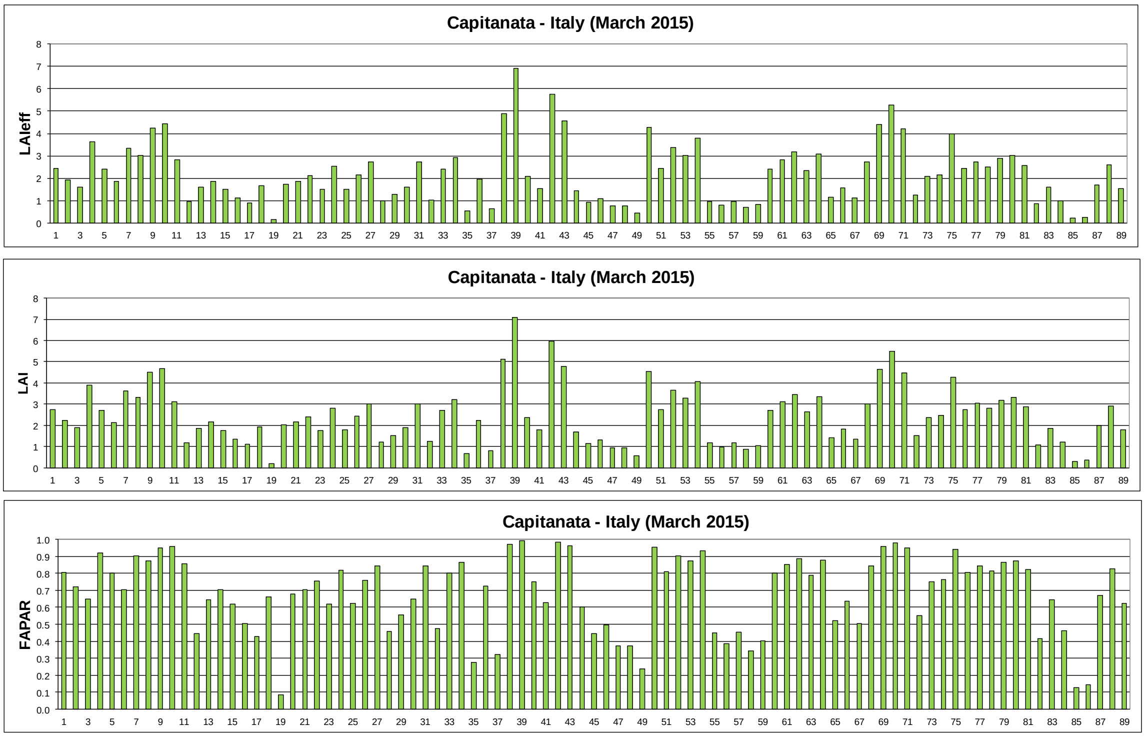

Figure 8: LAIeff, LAI and FAPAR measurements acquired in Capitanata site, during the field campaign in March, 2015.

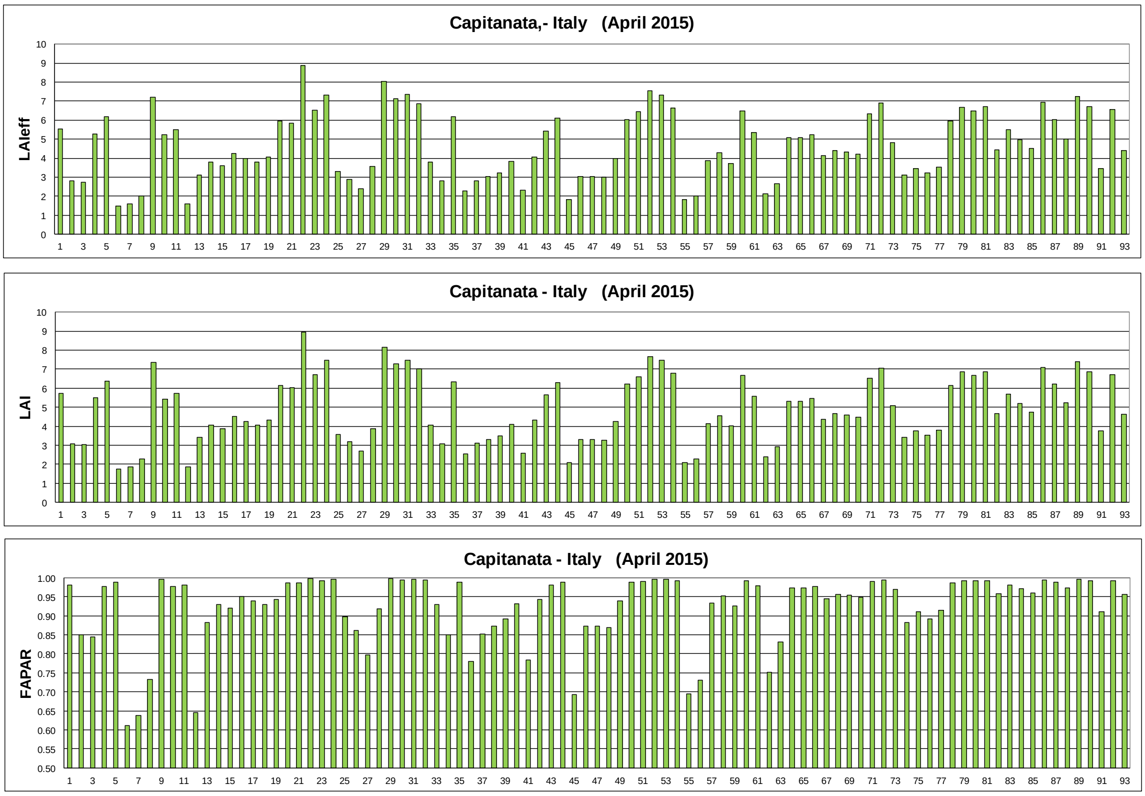

Figure 9: LAIeff, LAI and FAPAR measurements acquired in Capitanata site, during the field campaign April, 2015.

The distribution of the measured variables is presented in Figure 10 and Figure 11. A good distribution of values covering almost the whole dynamic range is obtained for the LAIeff and LAI, mainly for the second campaign. Note that the larger frequencies are obtained for highest vegetation values for the second campaign (April 2015) for FAPAR. For LAI and LAIeff, the first campaign ranges from zero to seven, and for the second one raises till eight.

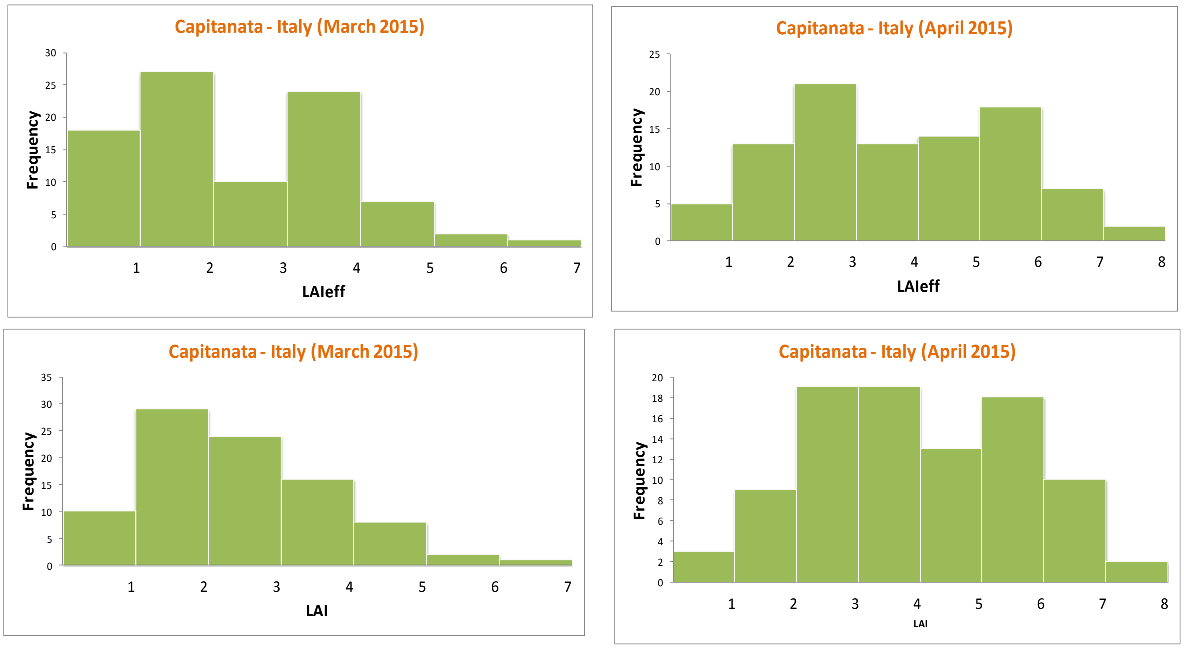

Figure 10: Distribution of the measured biophysical LAIeff and LAI variables over the ESUs, Capitanata site, during the field campaigns on 17th March and 23rd April, 2015.

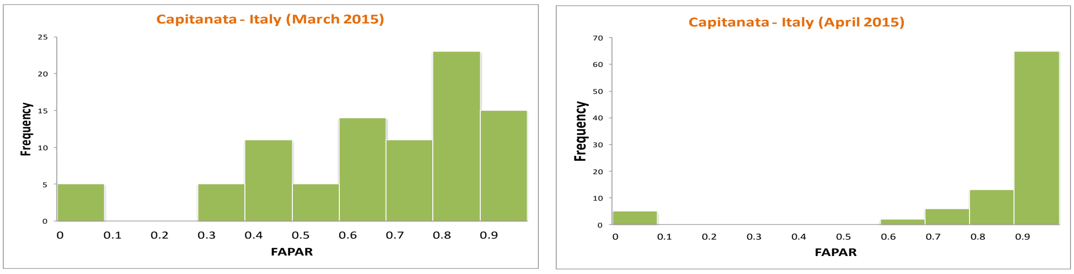

Figure 11: Distribution of the measured biophysical FAPAR variable over the ESUs, Capitanata site, during the field campaigns 17th March and 23rd April, 2015.

5. EVALUATION OF THE SAMPLING

5.1. PRINCIPLES

The data set sampling was concentrated in the most representative areas, the number of sampling points was 89 and 93, for the first and second field campaign respectively.

5.2. EVALUATION BASED ON NDVI VALUES

The sampling strategy is evaluated using the Landsat-8 image by comparing the NDVI distribution over the site with the NDVI distribution over the ESUs (Figure 12). As the number of pixels is drastically different for the ESU and whole site (WS), it is not statistically consistent to directly compare the two NDVI histograms. Therefore, the proposed technique consists in comparing the NDVI cumulative frequency of the two distributions by a Monte-Carlo procedure which aims at comparing the actual frequency to randomly shifted sampling patterns. It consists in:

1. computing the cumulative frequency of the *N* pixel NDVI that correspond to the exact ESU locations; then, applying a unique random translation to the sampling design (modulo the size of the image)
2. computing the cumulative frequency of NDVI on the randomly shifted sampling design
3. repeating steps 2 and 3, 199 times with 199 different random translation vectors.

This provides a total population of N = 199 + 1(actual) cumulative frequency on which a statistical test at acceptance probability 1 - α = 95% is applied: for a given NDVI level, if the actual ESU density function is between two limits defined by the $N\alpha/2 = 5$ highest and lowest values of the 200 cumulative frequencies, the hypothesis assuming that WS and ESU NDVI distributions are equivalent is accepted, otherwise it is rejected.

Figure 12 shows that the NDVI TOC distribution during the Capitanata for the second campaign (23rd April, 2015) is good over the whole site (10x10 km^2), a bias toward higher NDVI values is appreciated.

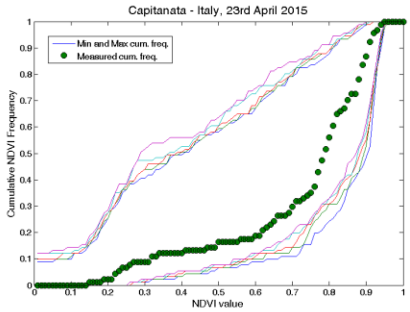

Figure 12: Comparison of NDVI TOC distribution between ESUs (green dots) and over the whole image (blue line). Capitanata site (2015). Second field campaign (23rd April).

5.3. Evaluation Based On Convex Hull: Product Quality Flag.

The interpolation capabilities of the empirical transfer function used for up-scaling the ground data using decametric images is dependent of the sampling (Martinez et al., 2009). A test based on the convex hulls was also carried out to characterize the representativeness of ESUs and the reliability of the empirical transfer function using the different combinations of the selected bands (green, red, NIR and SWIR) of the Landsat-8 image. A flag image is computed over the reflectances. The result on convex-hulls can be interpreted as:

- pixels inside the 'strict convex-hull': a convex-hull is computed using all the Landsat-8 reflectances corresponding to the ESUs belonging to the class. These pixels are well represented by the ground sampling and therefore, when applying a transfer function the degree of confidence in the results will be quite high, since the transfer function will be used as an interpolator;

- pixels inside the 'large convex-hull': a convex-hull is computed using all the reflectance combinations (±5% in relative value) corresponding to the ESUs. For these pixels, the degree of confidence in the obtained results will be quite good, since the transfer function is used as an extrapolator (but not far from interpolator);

- pixels outside the two convex-hulls: this means that for these pixels, the transfer function will behave as an extrapolator which makes the results less reliable. However, having a priori information on the site may help to evaluate the extrapolation capacities of the transfer function.

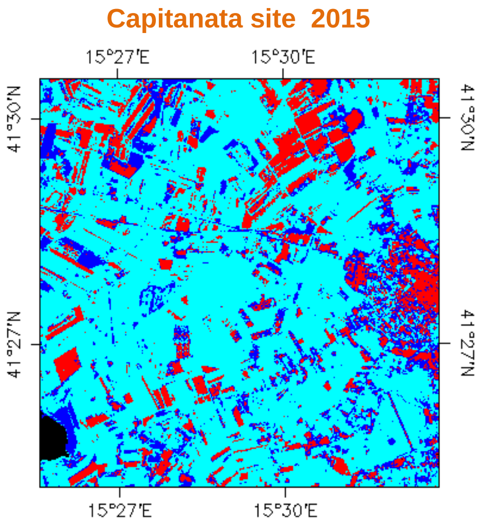

Figure 13: Convex Hull test over 10x10 km^2 area: clear and dark blue correspond to the pixels belonging to the 'strict' and 'large' convex hulls. Red corresponds to the pixels for which the transfer function is extrapolating and black to water areas, Capitanata 2015. Black corresponds to water areas . Second field campaign (23rd April).

Figure 13 shows the results of the Convex-Hull test (i.e., Quality Flag image) for the Capitanata site over a 10x10 km^2 area around the central coordinate site, performed during the second filed campign (23rd April, 2015). Large percentage values corresponding to the strict and large convex-hulls were found around the test site, with 85% over the 10x10 km^2 area and 90% for 5x5 km^2 area (see Table 3).

Table 3: Percentages of Convex hull results over the study areas (10x10 km2 and 5x5 km2) in Capitanata, 23rd April 2015. Convex hull values: 0= extrapolation of TF, 1= strict convex hull and 2= large convex hull.

Capitanata campaigns	Quality Flags (%)						
Field campaigns	5x5 km^2				10x10 km^2		
	0	1	2	1 & 2	0	1	2
23rd April 2015	10	80	10	90	15	70	15

The study area is focused over the 5x5 km^2 area around the central coordinate site. The large image of 100 km^2 includes a part of urban area (Foggia city) and the reservoir of Celone River. Several masks have been created in order to remove this water area, punctual clouds and shadows using the SWIR bands and NDVI. These pixels have been set to -1 for all the products. The area of 3x3 km^2 where the means values of biophysical maps have been calculated is clear and only includes crop fields.

6. PRODUCTION OF GROUND-BASED MAPS

6.1. IMAGERY

The Landsat-8 image was acquired for the second campaign on 30th April, 2015 (see Table 4 for acquisition geometry). We selected 4 spectral bands from 500 nm to 1750 nm with a nadir ground sampling distance of 30 m. For the transfer function analysis, the input satellite data used is Top of Canopy (TOC) reflectance. The original projection is UTM 33 North, WGS-84.

Table 4: Acquisition geometry of Landsat-8 data used for retrieving high resolution maps.

Landsat-8 TOC METADATA	
Platform / Instrument	Landsat-8 / OLI_TIRS
Path	189
Row	31
Selected Bands	B3(green) : 0.53-0.59 µm B4(red) : 0.64-0.67 µm B5(NIR) : 0.85-0.88 µm B6(SWIR1) : 1.58-1.66 µm
	Capitanata campaigns **23rd April 2015**
Acquisition date	2015.04.30 9:40:15
Illumination Azimuth angle	142.9278º
Illumination Elevation angle	58.3222º
Ground control points verify	215
Geometric RMSE Verify	5.563

6.2. THE TRANSFER FUNCTION

The measurements were collected in different dates that the acquisition dates of the Landsat-8 images used for the up-scaling. For this reason some measurements provided in the ground dataset present inconsistent values with the TOC reflectance and NDVI values of the satellite image. These measurements, corresponding to few ESUs, were not considered for the up-scaling.

6.2.1. The regression method

If the number of ESUs is enough, multiple robust regression 'REG' between ESUs reflectance and the considered biophysical variable can be applied (Martínez et al., 2009): we used the 'robustfit' function from the Matlab statistics toolbox. It uses an iteratively re-weighted least squares algorithm, with the weights at each iteration computed by applying the bi-square function to the residuals from the previous iteration. This algorithm provides lower weight to ESUs that do not fit well.

The results are less sensitive to outliers in the data as compared with ordinary least squares regression. At the end of the processing, two errors are computed: weighted RMSE (using the weights attributed to each ESU) (RW) and cross-validation RMSE (leave-one-out method) (RC).

As the method has limited extrapolation capacities, a flag image (Figure 13**Erreur ! Source du renvoi introuvable.**), based on the convex hulls, is included in the final ground based map in order to inform the users on the reliability of the estimates.

6.2.2. Band combination

Figure 14 shows the errors (RW, RC) obtained for the several band combinations using TOC reflectance for the second campaign. We have selected the NDVI as input for the transfer function (exponential relationship with LAI and linear relationship with FAPAR, see section 6.2.3). NDVI shows for FAPAR the lower errors over ESUs than other combinations and, for all parameters, assures a good consistency of the maps over the whole area and more confidence over ESU control points.

Capitanata site 2015

23rd April

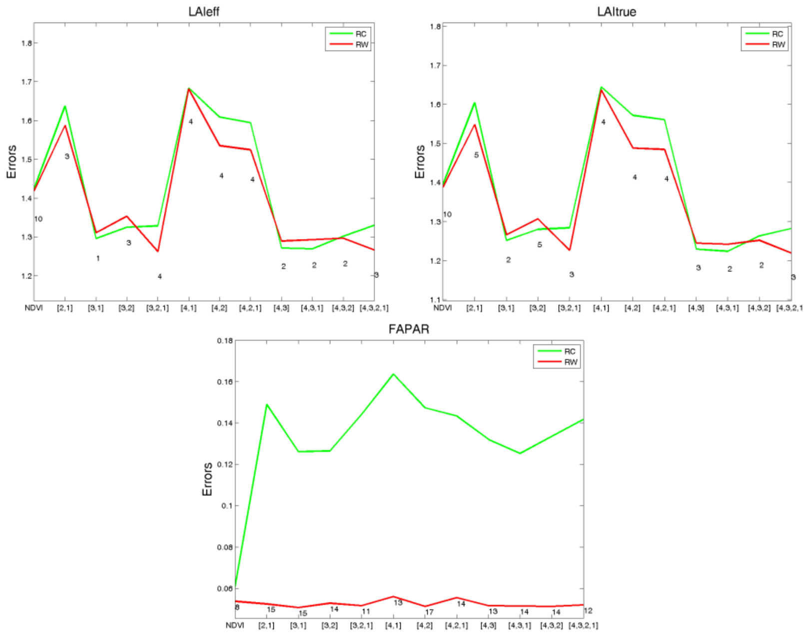

Figure 14: Test of multiple regression (TF) applied on different band combinations. Band combinations are given in abscissa (1=G, 2=RED, 3=NIR and 4=SWIR). The weighted root mean square error (RMSE) is presented in red along with the cross-validation RMSE in green. The numbers indicate the number of data used for the robust regression with a weight lower than 0.7 that could be considered as outliers. Capitanata 2015, field campaign on 23rd April.

6.2.3. The selected Transfer Function

The applied transfer function is detailed in Table 5, along with its weighted (RW) and cross validated (RC) errors.

For the FAPAR, a simple linear relationship with NDVI was selected:

$$FAPAR = a + b \cdot NDVI \qquad \text{Eq. (8)}$$

For the LAIeff and LAI, an exponential relationship with NDVI was selected according to Baret et al., (1989):

$$LAIeff = a + b \cdot ln\left(\frac{NDVI_{\infty} - NDVI}{NDVI_{\infty} - NDVI_S}\right) \qquad \text{Eq. (9)}$$

$$LAI = a + b \cdot ln\left(\frac{NDVI_{\infty} - NDVI}{NDVI_{\infty} - NDVI_S}\right) \qquad \text{Eq. (10)}$$

Where b represents the extinction coefficient which depends on the average leaf angle inclination, solar zenith angle and diffuse reflectance and transmittance of the leaves. "b" was set empirically with the ground data for each transfer function, as well as the residuals "a". $NDVI_S$ represents the typical NDVI of bare soil areas and $NDVI_{\infty}$ represents the NDVI of fully developed canopies, both assumed to be constant over the image. $NDVI_S$ was set to 0.22 and $NDVI_{\infty}$ to 0.95.

Table 5: Transfer function applied to the whole site for LAIeff, LAI and FAPAR. RW for weighted RMSE, and RC for cross-validation RMSE.

Variable	Band Combination	RW	RC
23rd April 2015			
LAIeff	$0.4477 - 2.001 \cdot ln\left(\frac{0.95-NDVI}{0.95-0.22}\right)$	1.40	1.42
LAI	$0.6581 - 2.0066 \cdot ln\left(\frac{0.95-NDVI}{0.95-0.22}\right)$	1.37	1.40
FAPAR	$0.0224 + 1.0922 \cdot NDVI$	0.06	0.05

Figure 15 shows scatter-plots between ground observations and their corresponding transfer function (TF) estimates for the selected bands combinations. A good correlation is observed for the LAIeff, LAI and FAPAR with points distributed along the 1:1 line.

Capitanata site 2015

23rd April

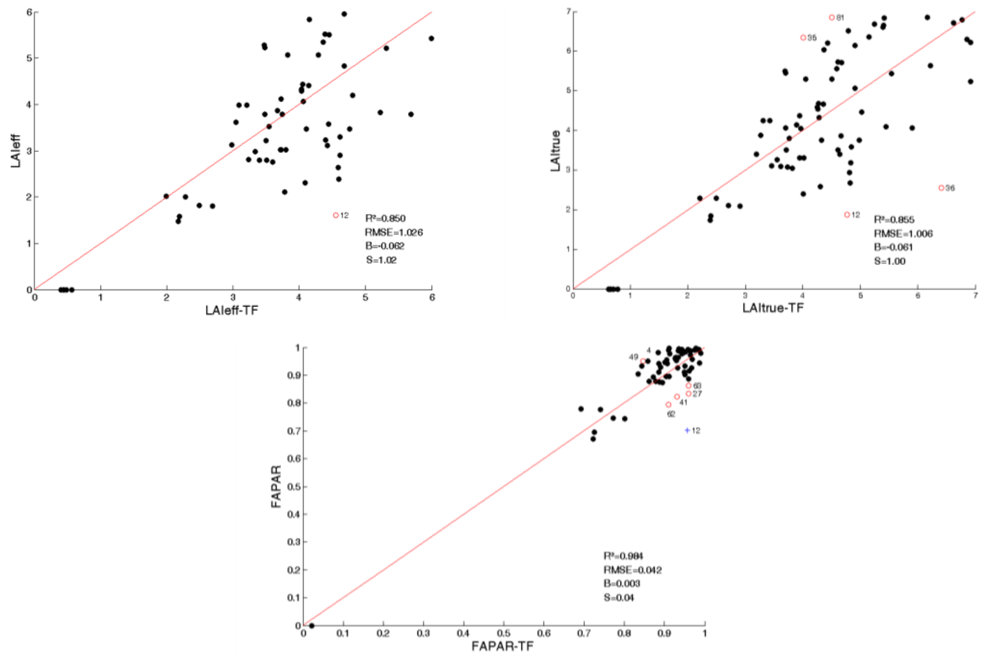

Figure 15: LAIeff, LAI and FAPAR results for regression on reflectance using the NDVI band. Full dots: Weight>0.7. Empty dots: 0<Weight<0.7. Crosses: Weight=0. Capitanata site, field campaign on 23rd April, 2015.

6.3. THE HIGH RESOLUTION GROUND BASED MAPS

The high resolution maps are obtained applying the selected transfer function (Table 6) to the Landsat-8 TOC reflectance. The study area has been extended to 10x10km^2 (centre located at 41.4637 N, 15.4867 E, UTM zone 33 North, Datum WGS-84). Figure 16 to Figure 18 present the TF biophysical variables over the extended 10x10 km^2 area. Figure 14 shows the Quality Flag included in the final product.

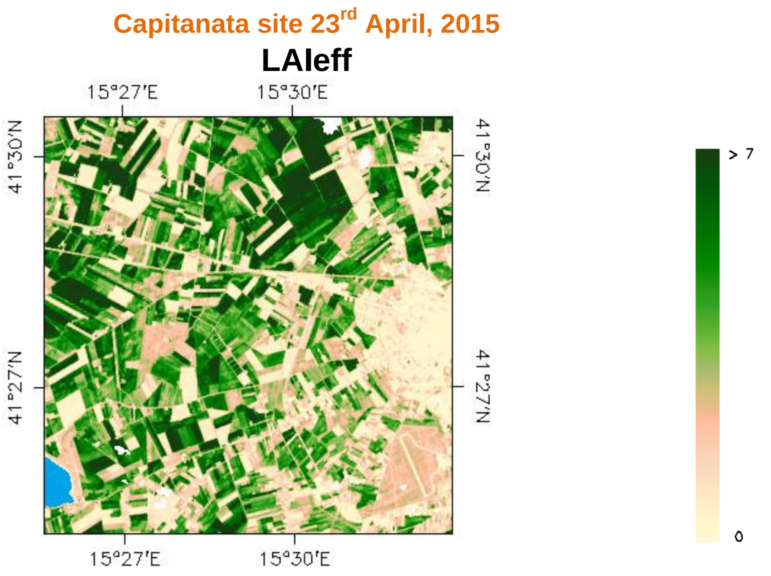

Figure 16: Ground-based Effective LAI maps (10x10 km^2) retrieved on *Capitanata site (Italy) 2015.* Second field campaign (23rd April).

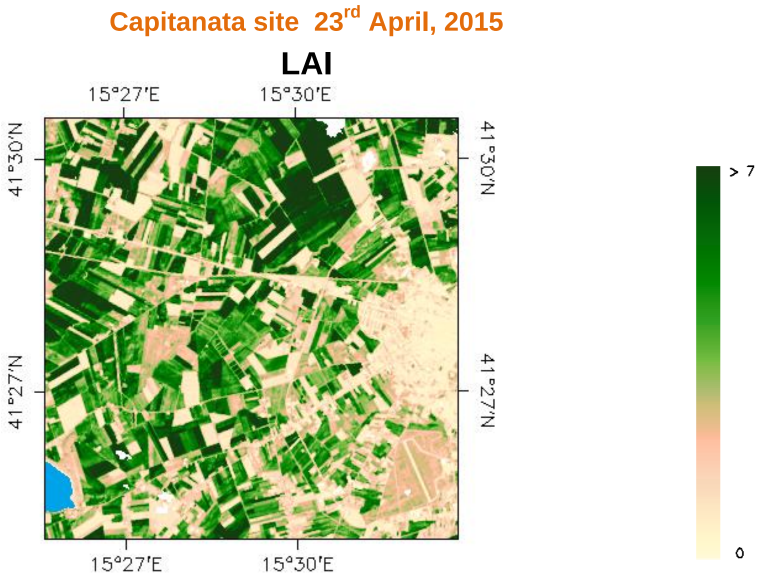

Figure 17: Ground-based LAI maps (10x10 km^2) retrieved on *Capitanata site (Italy) 2015.* Second field campaign (23rd April).

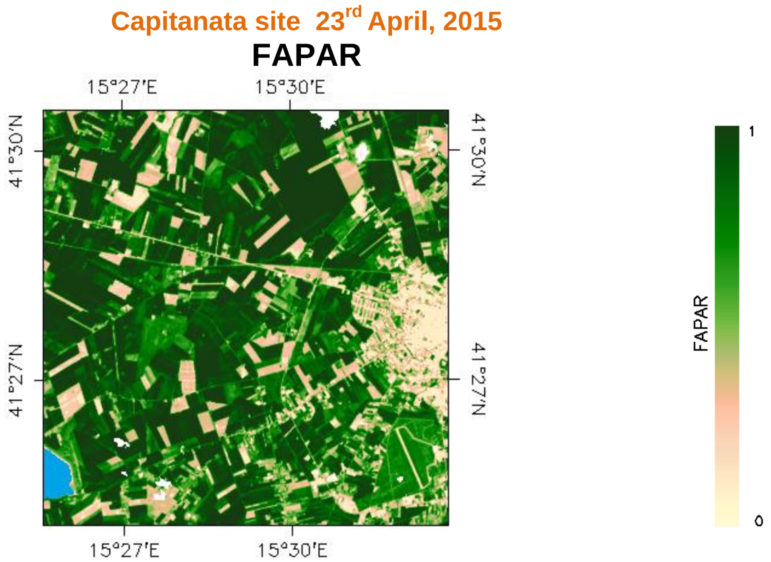

Figure 18: Ground-based of Instantaneous FAPAR maps (10x10 km^2) retrieved on *Capitanata site (Italy) 2015.* Right: Second field campaign (23rd April).

Figure 19 summarizes these ground-based high resolution maps over the 5x5 km^2 study area. These maps are provided for validation of satellite products at different resolutions (see Table 6).

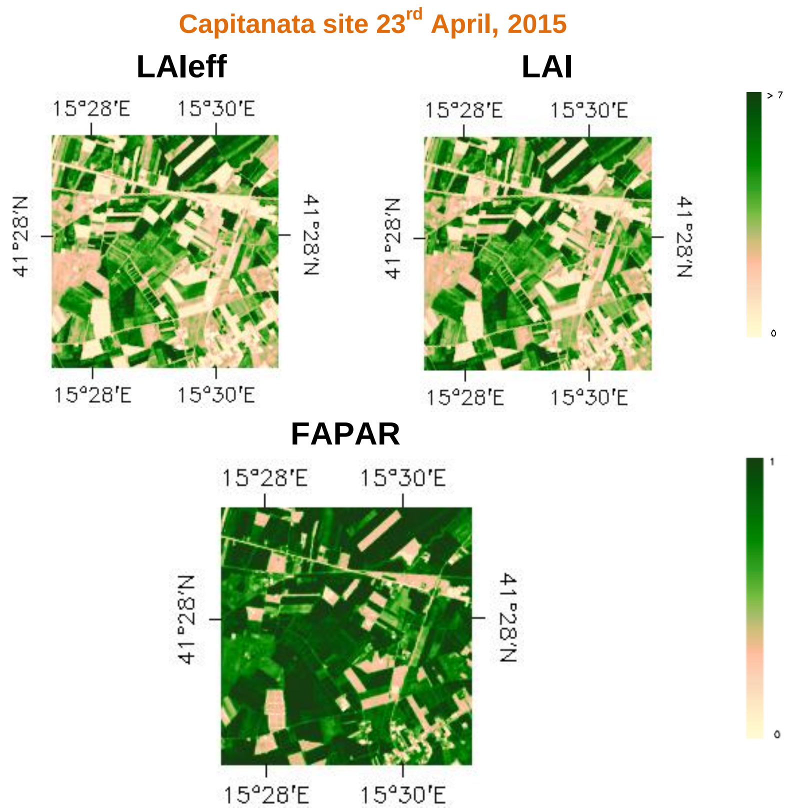

Figure 19: Ground-based maps (5x5 km^2) retrieved on Capitanata site (Italy). Second field campaign on 23rd April, 2015.

Figure 20 shows the scatter plot between biophysical variables that prove the good consistency of the 10x10 km^2 ground-based maps (all pixels), showing the exponential (LAI vs FAPAR) observed with the ground data. The most values are concentrated over higher values as we observed for the ground dataset.

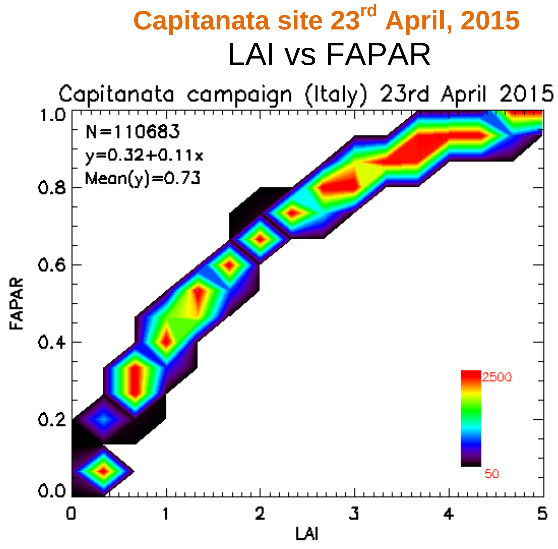

Figure 20: Scatter plots to LAI vs FAPAR for the two campaigns over *Capitanata site (Italy) 2015.* Second field campaign (23rd April).

6.3.1. Mean Values

Mean values of a 3x3 km^2 area centred in the test site are provided for the validation of 1 km satellite products in agreement with the CEOS OLIVE direct dataset (Table 6). For the validation of coarser resolutions product (e.g. MSG products) a larger area should be considered. For this reason, empirical maps are provided at 5x5 km^2 and 10x10 km^2.

Table 6: Mean values and standard deviation (STD) of the HR biophysical maps for the selected 3 x 3 km^2 area at Capitanata site (Italy) 2015.

3x3 km^2	Capitanata campaigns 2015					
	Mean Values			STDV Values		
	LAIeff	LAI	FAPAR	LAIeff	LAI	FAPAR
23rd April 2015	3.28	3.49	0.76	1.97	1.96	0.25

Table 7 describes the content of the geo-biophysical maps in the "BIO_YYYYMMDD_LANDSAT-8_Capitanata_ETF_Area" files.

Nomenclature: BIO_YYYYMMDD_SENSOR_Site_ETF_Area
where:

BIO stands for Biophysical (LAIeff, LAI and FAPAR)

SENSOR = LANDSAT-8

YYYYMMDD = Campaign date

Site = Capitanata

ETF stands for Empirical Transfer Function

Area = window size 10x10 and 5x5 km^2

Table 7: Content of the dataset.

Parameter	Dataset name	Range	Variable Type	Scale Factor	No Value
LAI effective	LAIeff	[0, 7]	Integer	1000	-1
LAI	LAI	[0, 7]	Integer	1000	-1
FAPAR 10:00 SLT	FAPAR	[0, 1]	Integer	10000	-1
Fraction of Vegetation Cover	FCOVER	[0, 1]	Integer	10000	-1
Quality Flag	QFlag	0,1,2,3 (*)	Integer	N/A	-1

(*) 0 means extrapolated value (low confidence), 1 strict interpolator (best confidence), 2 large interpolator (medium confidence), 3 mask for water areas.

7. CONCLUSIONS

The FP7 ImagineS project continues the innovation and development activities to support the operations of the Copernicus Global Land service. One of the JECAM sites is located in the northern part of Apulia Region (South-eastern Italy), the study is focused on an experimental farm situated in the middle of Capitanata plain within a flat topography (avg. Altitude 90 m) in Italy.

This report firstly presents the ground data collected during two field campaigns on 17th of March and 23rd of April, 2015. The dataset includes 89 and 93 elementary sampling units where LAIeff measurements were taken with the analyzer LAI2000 and LAI and FAPAR values were obtained with empirical relationships.

Clumping Factor was empirically determined using the using the Rinaldi and Garofalo, (2011) expression. Solar Global Radiation was collected with pyranometer. iPAR was estimated using Rinaldi and Garofalo, (2011) over the ESUs.

Secondly, high resolution ground-based maps of the biophysical variables have been produced over the site for the second campaign (23rd of April, 2015). Ground-based maps have been derived using high resolution imagery (Landsat-8 TOC Reflectance) according with the CEOS LPV recommendations for validation of low resolution satellite sensors. Transfer functions have been derived by multiple robust regressions between ESUs reflectance and the several biophysical variables. Due to the scene presents some heterogeneous zones as water and urban areas we have selected the NDVI as input for the transfer function (exponential relationship with LAIeff and LA, linear with FAPAR). NDVI assures good consistency of the maps over the whole area. The RMSE values for the several transfer function estimates are 1.03 for LAIeff, 1.01 for LAI, 0.04 for FAPAR.

The quality flag map based on the convex-hull analysis shows quite good quality (upper than 90% at 5x5 km^2 and 85% at 10x10 km^2).

The biophysical variable maps are available in geographic (UTM 33 North projection WGS-84) coordinates at 30 m resolution. Mean values and standard deviation for LAIeff, LAI, and FAPAR were computed over an area of 3x3 km^2 for validation of low and medium resolution satellite products.

8. ACKNOWLEDGEMENTS

This work is supported by the FP7 IMAGINES project under Grant Agreement N°311766. Landsat-8 Surface Reflectance HR imagery is provided through the USGS Global Visualization service. This work is done in collaboration with the consortium implementing the Global Component of the Copernicus Land Service.

Thanks to the CNR-SCA (*Consiglio Nazionale delle Ricerche - Unità di Ricerca per I Sistemi Colturali degli Ambienti caldo-aridi*) from Italy, for providing the field dataset in the context of JECAM program.

9. REFERENCES

Baret, F and Fernandes, R. (2012). Validation Concept. VALSE2-PR-014-INRA, 42 pp.

Baret, F., G. Guyot and Major, D. (1989). Crop biomass evaluation using radiometric measurements. Photogrammetria 43:241-256.

Camacho, F., Cernicharo, J., Lacaze, R., Baret, F., and Weiss, M. (2013). GEOV1: LAI, FAPAR Essential Climate Variables and FCOVER global time series capitalizing over existing products. Part 2: Validation and intercomparison with reference products. *Remote Sensing of Environment, 137: 310-329.*

Decagon Devices, Inc. (2014). AccuPAR PAR/LAI Ceptometer. Model LP80 manual. http://www.decagon.com

Demarez, V., Duthoit, S., Baret, F., Weiss, M. and Dedieu, G. (2008). Estimation of leaf area and clumping indexes of crops with hemispherical photographs. *Agricultural and Forest Meteorology. I48, 644-655*.

Fernandes, R., Plummer, S., Nightingale, J., et al. (2014). Global Leaf Area Index Product Validation Good Practices. CEOS Working Group on Calibration and Validation - Land Product Validation Sub-Group. *Version 2.0: Public version made available on LPV website*.

JECAM, (2014). GEO JECAM Progress Report 2015 (available online: http://www.jecam.org/images/uploads/sites/JECAM_Progress_Report_2014_.pdf)

JECAM, (2015). GEO JECAM Progress Report 2015 (available online: http://www.jecam.org/images/uploads/sites/JECAM_Progress_Report_2015_.pdf)

Lang A.R.G., (1986). Leaf area and average leaf angle from transmittance of direct sunlight. Australian Journal of Botany. 34: 349-355

Lang, A.R.G., (1987). Simplified estimate of leaf area index from transmittance of the sun's beam. Agricultural and Forest Meteorology. 41: 179-186

Latorre, C., Camacho, F., Castrignanò, A., De Benedetto, D., Stellacci, A.M., Ventrella, D., Campi, P., Rinaldi, M., Maddaluno, C., Mucci, M., Matese, A., Toscano, P. (2016). "Vegetation Field Data and Production of Ground-Based Maps: Capitanata site, Italy. 18th March and 13th May, 2014" report. (Available at ImagineS website: http://fp7-imagines.eu/pages/documents.php).

LI-COR Inc., Lincoln, Nebraska, (2013). http://envsupport.licor.com/docs/LAI-2000_Instruction_Manual.pdf.

Martínez, B., García-Haro, F. J., & Camacho, F. (2009). Derivation of high-resolution leaf area index maps in support of validation activities: Application to the cropland Barrax site. *Agricultural and Forest Meteorology, 149, 130–145*.

Miller, J.B. (1967). A formula for average foliage density. Aust. J. Bot., 15:141-144

Morisette, J. T., Baret, F., Privette, J. L., Myneni, R. B., Nickeson, J. E., Garrigues, S., et al. (2006). Validation of global moderate-resolution LAI products: A framework proposed within the CEOS land product validation subgroup. *IEEE Transactions on Geoscience and Remote Sensing, 44, 1804–1817*.

Nilson T. (1971). A theoretical analysis of the frequency of gaps in plant stands. Agricultural Meteorology 8, 25-38

Rinaldi, M., Garofalo, P., 2011. Radiation-use efficiency of irrigated biomass sorghum in a Mediterranean environment. Crop Pasture and Science, 62:830-839.